

# Magnetic Phases of Electron-Doped Manganites

G. Venkateswara Pai\*

Centre for Condensed Matter Theory, Department of Physics,  
Indian Institute of Science, Bangalore - 560012, India

We study the anisotropic magnetic structures exhibited by electron-doped manganites using a model which incorporates the double-exchange between orbitally degenerate  $e_g$  electrons and the super-exchange between  $t_{2g}$  electrons with realistic values of the Hund's coupling ( $J_H$ ), the super-exchange coupling ( $J_{AF}$ ), and the bandwidth ( $W$ ). We look at the relative stabilities of the G, C and A type antiferromagnetic phases. In particular we find that the G-phase is stable for low electron doping as seen in experiments. We find good agreement with the experimentally observed magnetic phase diagrams of electron-doped manganites ( $x > 0.5$ ) such as  $\text{Nd}_{1-x}\text{Sr}_x\text{MnO}_3$ ,  $\text{Pr}_{1-x}\text{Sr}_x\text{MnO}_3$ , and  $\text{Sm}_{1-x}\text{Ca}_x\text{MnO}_3$ . We can also explain the experimentally observed orbital structures of the C and A phases. We also extend our calculation for electron-doped bilayer manganites of the form  $\text{R}_{2-2x}\text{A}_{1+2x}\text{Mn}_2\text{O}_7$  and predict that the C-phase will be absent in these systems due to their reduced dimensionality.

PACS : 75.30.Vn, 75.30.Gw, 75.30.Et, 71.27.+a

## I. INTRODUCTION

Recently there has been a great upsurge of interest in doped manganites exhibiting colossal magnetoresistance. Most of the studies on manganites ( $\text{R}_{1-x}\text{A}_x\text{MnO}_3$ ;  $\text{R} = \text{La, Nd, Pr or Sm}$  and  $\text{A} = \text{Sr, Ca, Ba or Pb}$ ) focus on the transition from a ferromagnetic metal to a paramagnetic insulator in the doping regime  $0.15 < x < 0.4$  [1–3] which can be considered as doping the quarter filled  $e_g$  band of  $\text{RMnO}_3$  with holes. More recently, *electron-doped* manganites [4], namely systems with  $0.5 < x < 1$ , have begun to be explored. These seem to be different and quite interesting in their own way with a variety of anisotropic magnetic phases and with no evidence of *particle - hole symmetry*. Such systems are experimentally seen to exhibit A-type, C-type and G-type antiferromagnetism [5–7], spectacular transitions between these phases under an applied magnetic field [8] as well as possible phase separation. In contrast with the hole-doped systems, there have been very few attempts to understand the electron-doped systems theoretically. We show here that the rich magnetic phase diagram as well as their orbital structure can be understood in terms of a microscopic model which takes into account the *large but finite* Hund's rule *double-exchange* (DE) coupling, effects of orbital degeneracy and the *super-exchange* (SE) coupling between  $t_{2g}$  spins within a band picture.

We study this model in detail for realistic values of the Hund's coupling, the super-exchange coupling and the bandwidth. We present the phase diagram as a function of doping in reduced units of  $J_H/t$  and  $J_{AF}/t$ . From the phase diagram we deduce that the key interaction responsible for the stability of the G-phase near  $x = 1.0$  is the super-exchange interaction. We also find that the A-phase near  $x \sim 0.5$  is very sensitive to the variation of the super-exchange interaction. We obtain a G-type

phase for  $0.85 < x \leq 1$ , a C-type phase for  $0.6 < x \leq 0.85$  and an A-type phase for  $0.5 \leq x \leq 0.6$  for values of  $J_H$  (Hund's coupling),  $J_{AF}$  (super-exchange coupling) and  $t$  (hopping parameter) that are in agreement with density functional calculations [9]. Thus we find that a finite value of  $J_H$  leads to a magnetic phase diagram in good agreement with experiments for a number of doped manganites  $\text{R}_{1-x}\text{A}_x\text{MnO}_3$  for  $x > 0.5$ . The model also throws light on the nature of orbital occupation of the electronic degrees of freedom which will lead to the experimentally observed orbital ordering [6]. We extend the mean field theory to incorporate the CE-phase at  $x = 0.5$  and find that it is stabilized over a wide range of values of  $J_H S_0/t$  and  $J_{AF} S_0^2/t$ . We also use our model to make a number of predictions regarding the magnetic phases of electron-doped bilayer systems  $\text{R}_{2-2x}\text{A}_{1+2x}\text{Mn}_2\text{O}_7$  [10]. Specifically, we point out that the C-phase will be absent in the electron doped bilayer manganites due to reduced dimensionality.

We start by briefly describing the experimental situation. In Section II we present our model. In Sections III we present our results on the magnetic phase diagram of the manganites. Section IV deals with the nature of the G-phase for low electron doping and of canting of spins. In Section V we explain the orbital structures observed in the C and A phases. Section VI deals with the phase diagram of the electron-doped bilayer manganites. Finally we make a comparison of our results with the earlier works and point out the shortcomings of various approaches including ours.

The conventional single-band double exchange model predicts a phase diagram symmetric about  $x = 0.5$ . However, the behaviour of the observed ground state magnetic properties does not agree this simple picture. Experiments show a remarkable asymmetry with re-

gard to the magnetic properties of the system. In  $La_{1-x}Sr_xMnO_3$  an A - type antiferromagnetic ground state is seen for  $0.52 < x < 0.58$ , above which it becomes a C-type antiferromagnet. In  $Nd_{1-x}Sr_xMnO_3$  an A-type antiferromagnetic phase extends from  $x \sim 0.5$  to  $x \sim 0.62$  and a C-type phase is seen till  $x \sim 0.8$  [6]. In  $Pr_{1-x}Sr_xMnO_3$  the A-type antiferromagnetism is seen from  $x \sim 0.48$  upto  $x \sim 0.6$  and the C-antiferromagnetism upto  $x \sim 0.9$  [5]. The end compound  $AMnO_3$  is a G-type antiferromagnet and this state extends, in general, upto  $x \sim 0.90$  [11]. In particular, recent experiments on  $Sm_{1-x}Ca_xMnO_3$  suggests that the G-phase, albeit with ferromagnetic clusters embedded in them, survives upto a doping concentration of  $x = 0.88$  [12]. Though a picture based on band-structure will not be appropriate in such a case, we believe that the nature of the background magnetic phase can still be captured since the dominant energy here is the antiferromagnetic energy resulting from the super-exchange.

## II. MODEL

If one starts from  $AMnO_3$  and increase the doping, the doped electrons go into empty  $e_g$  levels doubly degenerate in the absence of Jahn-Teller splitting. As noted in [13,14] the double-exchange between these degenerate  $e_g$  levels along with the super-exchange between  $t_{2g}$  core spins lead to a qualitatively different phase diagram which is highly asymmetric about  $x = 0.5$ . However, the resulting  $T = 0$  phase diagram they obtained while asymmetric is in disagreement with experiments on several counts (see below). This motivates a detailed study of an orbitally degenerate double-exchange(DE) and super-exchange(SE) model for  $0.5 < x < 1$  with realistic values of parameters  $J_H, J_{AF}$  and bandwidth  $W$  [15]. The effective Hamiltonian describing the low energy properties of the system is

$$H = J_{AF} \sum_{\langle ij \rangle} \mathbf{S}_i \cdot \mathbf{S}_j - J_H \sum_{i,\alpha,\mu,\mu'} \mathbf{S}_i \cdot c_{i\alpha\mu}^\dagger \vec{\sigma}_{\mu\mu'} c_{i\alpha\mu}' - \sum_{\langle ij \rangle, \mu} t_{ij}^{\alpha\beta} c_{i\alpha\mu}^\dagger c_{j\beta\mu} \quad (1)$$

Here  $\alpha$  and  $\beta$  denote the  $d_{3z^2-r^2}$  and  $d_{x^2-y^2}$  orbitals respectively,  $S_i$  is the  $t_{2g}$  spin at site  $i$ ,  $J_H$  is the Hund's coupling and  $J_{AF}$  the super-exchange between  $t_{2g}$  spins at nearest - neighbour sites  $i$  and  $j$ , and  $\mu$  stands for the spin degree of freedom of the itinerant electrons. The hopping matrix elements are determined by the symmetry of  $e_g$  orbitals [16].

We treat the spin subsystem quasiclassically. Assuming a homogeneous ground state we take  $\mathbf{S}_i = \mathbf{S}_0 \cos(\vec{Q} \cdot \vec{r}_i)$ . where  $\vec{Q} = (0, 0, 0)$  for the ferromagnetic phase,  $\vec{Q} = (\pi, \pi, \pi)$  for the G-type antiferromagnetic

phase,  $\vec{Q} = (\pi, \pi, 0)$  for the C-type antiferromagnetic phase, and  $\vec{Q} = (0, 0, \pi)$  for the A-type antiferromagnetic phase. Canting can be included by assuming  $\mathbf{S}_i = S_0(\sin \theta_i, \sin \theta_i, \cos \theta_i)$  with  $\theta_i$  taking values between 0 and  $\pi$ . This is discussed late below [17].

Under these assumptions the electronic part of the Hamiltonian reduces to

$$H_{el} = \sum_{k,\alpha,\beta} \epsilon_k^{\alpha\beta} c_{k\alpha\uparrow}^\dagger c_{k\beta\uparrow} + \sum_{k,\alpha,\beta} \epsilon_k^{\alpha\beta} c_{k\alpha\downarrow}^\dagger c_{k\beta\downarrow} - \frac{J_H S_0}{2} \sum_{k,\alpha} c_{k\alpha\uparrow}^\dagger c_{k+Q\alpha\uparrow} - \frac{J_H S_0}{2} \sum_{k,\alpha} c_{k\alpha\uparrow}^\dagger c_{k-Q\alpha\uparrow} + \frac{J_H S_0}{2} \sum_{k,\alpha} c_{k\alpha\downarrow}^\dagger c_{k+Q\alpha\downarrow} + \frac{J_H S_0}{2} \sum_{k,\alpha} c_{k\alpha\downarrow}^\dagger c_{k-Q\alpha\downarrow} \quad (2)$$

with [16]

$$\begin{aligned} \epsilon_{11} &= -\frac{2}{3}t(\cos k_x + \cos k_y) - \frac{8}{3}t \cos k_z, \\ \epsilon_{12} = \epsilon_{21} &= -\frac{2}{\sqrt{3}}t(\cos k_x - \cos k_y) \\ \epsilon_{22} &= -2t(\cos k_x + \cos k_y). \end{aligned} \quad (3)$$

The super-exchange contribution to the Hamiltonian is given by

$$H_{SE} = \frac{J_{AF} S_0^2}{2} (2 \cos \theta_{xy} + \cos \theta_z) \quad (4)$$

with  $\theta_{xy} = \theta_z = 0$  for ferromagnetic,  $\theta_{xy} = \theta_z = \pi$  for the G -type antiferromagnetic,  $\theta_{xy} = \pi$  and  $\theta_z = 0$  for the C -type antiferromagnetic, and  $\theta_{xy} = 0$  and  $\theta_z = \pi$  for the A -type antiferromagnetic phases. Here  $\theta_{xy}$  is the angle between nearest neighbour spins in the  $x$ - $y$  plane, and  $\theta_z$  is the angle between nearest neighbour spins in the  $z$  direction. Inclusion of canting by assuming  $\mathbf{S}_i = S_0(\sin \theta_i, \sin \theta_i, \cos \theta_i)$  will connect different spin species at the same site. These contributions come from the  $\sigma_x$  and  $\sigma_y$  terms in the DE part of the Hamiltonian which are absent when canting is absent. Thus the DE part of the Hamiltonian becomes

$$\begin{aligned} H_{DE} &= -J_H S_0 \sum_{j,\alpha} \cos \theta_j (c_{j\alpha\uparrow}^\dagger c_{j\alpha\uparrow} - c_{j\alpha\downarrow}^\dagger c_{j\alpha\downarrow}) \\ &- J_H S_0 \sum_{j,\alpha} \sin \theta_j (c_{j\alpha\uparrow}^\dagger c_{j\alpha\downarrow} + c_{j\alpha\downarrow}^\dagger c_{j\alpha\uparrow}) \\ &+ J_H S_0 \sum_{j,\alpha} i \sin \theta_j (c_{j\alpha\uparrow}^\dagger c_{j\alpha\downarrow} - c_{j\alpha\downarrow}^\dagger c_{j\alpha\uparrow}) \end{aligned} \quad (5)$$

We have neglected the correlation term in the Hamiltonian  $U \sum_{i\alpha} n_{i,\alpha\uparrow} n_{i,\alpha\downarrow} + V \sum_{i,\sigma,\nu} n_{i,1,\nu} n_{i,2,\sigma}$  and the Jahn - Teller contribution  $g \sum_{i,\alpha,\beta,\sigma} c_{i,\sigma,\alpha}^\dagger \mathbf{Q}_i^{\alpha\beta} c_{i,\sigma,\beta}$  with  $\mathbf{Q}$  describing the local distortion which lifts the degeneracy [18]. We neglect the correlation term because of the

low electron doping regime we are interested in. ( $x = 0.5$  refers to a filling of 0.125 in our model and the filling ranges from 0 to 0.125). For the same reason the inter-site Coulomb correlations, which may be necessary for the stability of charge ordered phase around  $x = 0.5$ , are also neglected. A cooperative Jahn-Teller effect can drastically change the magnetic ground state [19]. However, since the carrier concentration is very small, so is the *effective number of Jahn - Teller centres* and hence we do not expect any qualitative change in the magnetic phase diagram though both may be required alongwith the breathing mode distortions induced by holes to explain the CE - type charge ordered phase at  $x = 0.5$  [20]. Doping-induced disorder can have two effects. Firstly substitutional disorder may localize  $e_g$  electrons. However as long as the localization length is more than the inter atomic spacing, the hopping to nearest neighbour sites will split the energy levels into bonding and anti-bonding orbitals with electrons occupying the bonding orbitals. This process is naturally taken care of in our model. Secondly the presence of a magnetic rare-earth ion can have coupling with the magnetic  $Mn^{3+}$  ion and thus leading to change in the Mn-RE coupling as doping varies. However in most of the manganites, the RE ion in general is non-magnetic (*eg. La*) except, say in Pr. However studies on Pr-Sr system around  $x = 0.37$  [21] have shown that Mn-Pr coupling plays no role in the magnetic properties. Hence we also do not expect substitutional disorder to play a role in determining the magnetic phases though, as argued in [13,14], it might play a role in the transport properties of these compounds. We obtain the magnetic phase diagram by minimizing the total energy  $H_{el} + H_{SA}$  as a function of filling by fixing the chemical potential.

We present the magnetic phase diagram for both manganites and bilayer manganites as a function of  $J_H/t$  and  $J_{AF}/t$ . From density functional studies [9] we estimate  $t = 0.15\text{eV}$ ,  $J_H S = 0.75\text{eV}$  and  $J_{AF} S^2 = 8\text{meV}$ . Hence, we choose  $J_H S_0/t = 5$  and  $J_{AF} S_0^2/t = 0.053$ . This value of  $J_{AF} S_0^2/t$  also leads to the correct mean field  $T_N$  for the end compound  $\text{CaMnO}_3$ . Hence we use the phase diagram corresponding to these values for making comparison with experiments [22].

### III. PHASE DIAGRAM OF THE ELECTRON DOPED MANGANITES

The  $x = 1$  limit corresponds to empty  $e_g$  orbitals. The only contribution to the Hamiltonian comes from the SE interaction which is isotropic and hence leads to the G-phase at  $x = 1$ . At low electron doping, however, the SE still wins over the Hund's coupling and leads to the G-phase.

Doped electrons go into states with minimal energy corresponding to the  $\Gamma$  point at  $\mathbf{k} = 0$ . (This is a consequence of the band-picture we, as well as other workers, use. The possibility of the doped electron forming ferromagnetic clusters is mentioned later, in which case the band-picture will break down.) We first assume that all doped charges go into the state with  $\mathbf{k} = 0$  and neglect for the moment the effects due to finite filling of the bands. (Strictly speaking this is only the case for very small doping). Assuming uncanted states the energies for various magnetic states at  $\mathbf{k} = 0$  are

$$E_G = -3J_{AF}S_0^2/2t - y\sqrt{16 + (J_H S_0/2t)^2}, \quad (6)$$

$$E_A = J_{AF}S_0^2/2t - 4y - J_H S_0 y/2t, \quad (7)$$

$$E_C = -J_{AF}S_0^2/2t - 8y/3 - y\sqrt{16/9 + (J_H S_0/2t)^2}, \quad (8)$$

$$E_F = 3J_{AF}S_0^2/2t - 4y - J_H S_0 y/2t. \quad (9)$$

Here  $y$  is the actual electron filling in the two band model and is related to  $x$  as  $x = -4y + 1$ . For  $J_H S_0/t = 5$  and  $J_{AF} S_0^2/t = 0.053$  we find that the G-phase is stable upto  $x = 0.76$  beyond which the A-phase becomes stable. In Fig(1) we present the phase diagram assuming the electrons go into the  $\Gamma$  point and there is no canting of core spins. We plot the phase diagram as a function of doping and  $J_{AF} S_0^2/t$  for a fixed value of  $J_H S_0/t = 5$  and doping and  $J_H S_0/t$  for a fixed value of  $J_{AF} S_0^2/t = 0.053$ .

The effects due to finite band-filling will alter these values and the numerically obtained values can be read from Fig(2) and Fig(3). This also leads to the physically expected result that the doping region over which the G-phase stabilizes grows with  $J_{AF}/t$ . As electron doping increases the kinetic energy starts dominating over the SE contribution leading to increased spin alignment. This happens because kinetic energy is an increasing function of doping and for small doping it is proportional to the electron filling. However, a three-dimensional antiferromagnetic spin alignment does not allow for the motion of electrons. So to take advantage of the kinetic energy gain the mobile electrons polarize the spins along chains, planes and finally in all three directions successively. The reduction in the DE energy due to such alignment is overcome by the gain in kinetic energy beyond some doping value (for given values of  $J_H/t$  and  $J_{AF}/t$ ) and this point defines the G-C phase boundary. Moreover, as we will see in the next section, the C-phase has orbital ordering of  $d_{z^2}$ -type and the A-phase has orbital ordering of  $d_{x^2-y^2}$ -type. Thus the interplay of the spin alignment along chains or planes and the corresponding orbital order also leads to change of the '*effective hopping parameters*',  $t_z$  and  $t_{xy}$ , in the  $z$  and  $x - y$  directions. In general, this leads to the system transforming from one-dimensional, to two-dimensional and finally three dimensional ferromagnetic structures with increasing doping. Thus the competition between *effective kinetic energy* (determined by  $J_H$  and band

filling) and *super-exchange* leads to transitions G-C-A-F (with number of antiferromagnetic bonds 6, 4, 2 and 0 respectively) as the doping is varied for a given  $J_H/t$ .

In Fig(2) we present the results for  $J_H S_0/t = 5$ . For  $J_{AF} S_0^2/t = 0.053$  we find that the system has a stable ferromagnetic ground state upto  $x = 0.47$ , the A-phase is favoured for  $x < 0.57$ , the C-phase upto 0.85. The G-phase becomes the stable phase for  $0.85 < x < 1$ . We also find that the A - phase near  $x = 0.5$  is stable only for a limited range of  $J_{AF} S_0^2/t$ . The overall phase diagram is in excellent agreement with the experimentally observed phase diagram of NdSr, PrSr and SmCa systems.

In Fig(3) we present the results for  $J_{AF} S_0^2/t = 0.053$ . We find that the A-phase, stable near  $x = 0.5$  for smaller values of  $J_H S_0/t$ , gets pushed to the right making the ferromagnetic state stable near  $x = 0.5$  for large values of  $J_H/t$ . However, in contrast to the earlier case, the A - phase is stable over a wide range of values of  $J_H S_0/t$ . We conclude that the A - phase near  $x = 0.5$  is very sensitive to the variation of  $J_{AF} S_0^2/t$  and rather less sensitive to the variation of  $J_H S_0/t$ .

At  $x = 0.5$  most of the manganites have a charge/orbital ordered ground state with the magnetic phase being the CE-type antiferromagnet. Our mean field theory can be extended to include the uncanted CE phase by assuming  $\mathbf{S}_i = \mathbf{S}_0/2 (\cos(\vec{Q}_1 \cdot \vec{r}_i) - \cos(\vec{Q}_2 \cdot \vec{r}_i) + \cos(\vec{Q}_3 \cdot \vec{r}_i) + \cos(\vec{Q}_4 \cdot \vec{r}_i))$  with  $\vec{Q}_1 = (\pi, 0, \pi)$ ,  $\vec{Q}_2 = (0, \pi, \pi)$ ,  $\vec{Q}_3 = (\pi/2, 3\pi/2, \pi)$  and  $\vec{Q}_4 = (3\pi/2, \pi/2, \pi)$ . We present the phase diagram at  $x = 0.5$  as a function of  $J_H S_0/t$  and  $J_{AF} S_0^2/t$  in Fig(4). We find that at  $J_H S_0/t = 5$  and  $J_{AF} S_0^2/t = 0.053$ , the CE phase stabilizes over other phases. In fact, the CE phase is stabilized over a wide region of the phase diagram at  $x = 0.5$ . This may explain why most of the manganites at  $x = 0.5$  have the CE phase as the magnetic ground state. However, it is to be noted that the CE phase we obtain is not charge/orbital ordered. Other interaction such as the strong Coulomb repulsion or coupling of the lattice degrees of freedom to the  $e_g$  electrons may be needed to make this phase charge/orbital ordered. There are contrasting views regarding the origin of the charge/orbital ordered CE phase and the precise role of JT and Coulomb effects is still not clear. Strong on-site Coulomb correlations within a two-band model seem to stabilize the CO phase at  $x = 0.5$  [23]. It can also be thought of as emerging due to the doping dependent Berry phase associated with the JT effect [24]. However, manganites at  $x = 0.5$  exhibit a variety of ground states including the CE phase as in PrCa or NdSr, the A-phase as in PrSr or the metallic ferromagnetism as in LaSr. A Monte-Carlo study of the two-band model with JT phonons [25] seem to capture most of these phases. An extension of our mean field theory incorporating the

Jahn-Teller effect and breathing mode reproduces the charge/orbital ordered CE phase as well as the A-type phase [20].

#### IV. THE NATURE OF THE G-PHASE AND CANTING

Experimentally [5], [6] it is seen that there seems to be little canting in the A and C phases. This was also emphasized by Maezono *et. al.* [13]. It is also seen that there is a predominant occupation of orbitals of one character in these phases. Recent experiments by Mahendiran *et. al.* [12] on  $\text{Sm}_{1-x}\text{Ca}_x\text{MnO}_3$  suggest that even the G-phase for low doping may have little canting. The doped carriers seem to form ferromagnetic clusters leaving behind a uniform G-phase as background. In the band-picture, we have already noticed that for low electron doping the SE wins over the DE and the phase is G-type antiferromagnetic. One expects this phase to be canted as electrons gain kinetic energy due to the DE mechanism. The canting angle will be anisotropic, i.e.,  $\theta_{xy}$  will be different from  $\theta_z$  due to the anisotropy of the hopping integrals  $t_{\alpha\beta}^{ij}$ . However, no specific orbital ordering can be seen in this phase. This phase (without any orbital ordering) also has to be contrasted to the A-phase near  $x = 0.5$  which has orbital ordering of  $d_{x^2-y^2}$  type (see next section). The stability of the G-phase near  $x = 1$  is because of the dominance of antiferromagnetic energy whereas the stability of the A-phase near  $x = 0.5$  arises from the kinetic energy gain through DE in the plane due to selective  $d_{x^2-y^2}$  orbital ordering. Moreover, for finite  $J_H$  the canting is relatively small leading to a phase which closely resembles the G-phase at  $x = 1$ . In Fig(5) we plot the canting angles as a function of  $J_H/t$  for a fixed value of  $J_{AF}/t$  for some representative value of doping ( $x = 0.98$ ). We find that the canting angle increases as a function of  $J_H/t$  for a given filling and  $J_{AF}/t$  near  $x = 1$ .

In the limit  $J_H \rightarrow \infty$ , electron hopping to neighbouring sites with antiparallel core spins is not allowed. This is because the ‘effective hopping parameter’ for  $J_H \rightarrow \infty$  is proportional to  $t \cos(\theta/2)$  where  $\theta$  is the angle between the spins at neighbouring sites and antiparallel arrangement of spins reduces the ‘effective hopping parameter’ to zero. Hence the only way the electrons can take advantage of the kinetic energy gain due to increased doping is by canting the spins as much as possible. However, since  $t_{ij}$ ’s are anisotropic the canting angles will also be anisotropic. For a representative value of electron doping ( $x = 0.98$ ) we find that there is no canting in the  $z$  direction and spins cant by about  $10^\circ$  in the  $x - y$  plane. This gives rise to a net ferromagnetic moment in the plane with a value higher than that across the

layers. Hence one would think of it as a canted A-phase as in [14]. However, inclusion of finite  $J_H$  changes this picture. A finite value of  $J_H$  allows the spins to go to ‘*wrong spin state*’ at neighbouring site with an energy cost  $J_H$ . Hence the canting angle is reduced drastically compared to the  $J_H \rightarrow \infty$  limit. In fact, for experimentally realistic values of  $J_H$  the canting is almost absent for low electron doping as can be inferred from Fig(5). (In fact one expects no canting for  $J_H = 0$  as DE is not operative.) Moreover, the kinetic energy gain which is proportional to the doping is also not effective in overcoming the SE energy. Hence one gets a canted G-phase with very small canting angles, thus resembling the G-phase at  $x = 1$ . Since the kinetic energy gain is also very small due to the smallness of the canting angle, this phase does not have any preferential orbital arrangement of the  $d_{z^2}$  or  $d_{x^2-y^2}$  type as in the C and A phases. Thus we find that the stability of the G-phase is mainly due to the dominance of SE energy. This also means that the doping region over which the G-phase stabilizes will grow with increase in  $J_{AF}/t$ . In particular, for  $J_{AF}/t = 0$  the system should exhibit ferromagnetism for any doping making the G-C phase boundary collapse to the  $x = 1$  point in the  $J_{AF}/t$ - $x$  phase plane. However [14] find that the phase boundary between the canted G-phase and the C-phase does not change significantly as  $J_{AF}/t$  is varied. More surprisingly, their phase diagram, if extrapolated to  $J_{AF}/t = 0$ , will give the canted A-phase over a small region of doping near  $x = 1$ . In contrast to this, our phase diagram gives a ferromagnetic state for  $J_{AF}/t = 0$  for the whole doping regime and the stability region of the G-phase grows with increase in  $J_{AF}/t$  in agreement with the physically expected result. Our results agree in general with the results of Maezono *et. al* [13] though the A-phase near  $x \sim 0.5$  is missing in that work. Sheng and Ting [26] considered the problem from the strong correlation limit in contrast to the band limit which we have adopted. The C-phase between  $x = 0.6$  and  $x = 0.9$  is missing in the strong correlation limit.

## V. ORBITAL STRUCTURE

We find that in the C-phase the occupied orbitals are predominantly of  $d_{z^2}$  character with a small admixture of  $d_{x^2-y^2}$ . This happens because the electrons gain kinetic energy along the direction in which ferromagnetic correlations are stronger. For the same reason we find that in the A-phase the occupied orbitals are predominantly of  $d_{x^2-y^2}$  character. This, in effect, leads to suppression of hopping along antiferromagnetic bonds and explains why there is little canting in these systems. This is in agreement with experiments on  $\text{Nd}_{1-x}\text{Sr}_x\text{MnO}_3$  [6]. This also leads to a highly anisotropic band structure for G, C and A type structures and this feature becomes sharper as

$J_H$  increases. In particular, the C-phase has a quasi-one dimensional density of states. This also makes this phase very sensitive to substitutional disorder, possibly making it insulating. However, the A-phase is not sensitive to disorder and this rationalizes the (in-plane) metallic A-phase seen in experiments [5]. The nature of the occupied orbitals prevents electron motion along the  $z$  direction giving rise to a large anisotropy in the in-plane and out-of-plane resistivities. Experiments which probe the density of states, like tunneling measurements, will be able to see this feature. The low-temperature magnon spectrum will also throw light on the precise nature of the antiferromagnetic phase near  $x = 1$  and specifically the nature of canting in different manganites.

## VI. PHASE DIAGRAM OF THE ELECTRON DOPED BILAYER MANGANITES

The present scheme of calculation can also be applied to electron - doped bilayer manganites such as  $R_{2-2x}A_{1+2x}Mn_2O_7$  about which very little is known [10]. Since the interlayer coupling is roughly two orders of magnitude smaller than the coupling between bilayers one can apply the degenerate double - exchange, super - exchange model for a two layer system to study bilayered manganites. In this case the Brillouin zone is modified with  $k_z$  taking only two values. As noted earlier the magnetic structure depends on the competition between the super-exchange and the kinetic energy renormalized by magnetic structure and orbital degrees of freedom. This suggests that in bilayer compounds where the kinetic energy gain is predominantly in planes than in the  $z$  direction, the A-type antiferromagnetic phase is stabilized over the C-phase. This means that the dimensionality of the system plays a crucial role in the stability of the C-phase. This can be clearly seen in the limit  $J_H \rightarrow \infty$  where the band structure for C-phase becomes one dimensional with  $\epsilon = -\frac{8}{3}t \cos(k_z)$ . Detailed calculations support this picture as seen in Fig(6) where we present the results for a fixed value of  $J_H S/t = 5$  and in Fig(7) where we present the results for a fixed value of  $J_{AF} S^2/t = 0.053$ . Battle *et. al.* [27] have reported an A-type phase for  $\text{NdSr}_2\text{Mn}_2\text{O}_7$  ( $x = 0.5$ ) and  $\text{Nd}_{1.1}\text{Sr}_{1.9}\text{Mn}_2\text{O}_7$  ( $x = 0.45$ ). We believe that this phase should extend even beyond  $x = 0.5$  in accordance with our picture. Our phase diagram is in accordance with that of Maezono and Nagaosa [28]

## VII. DISCUSSION

It is interesting to study the phase transitions between these anisotropic structures under an applied magnetic

field in  $z$  direction. We find that the G-type phase becomes a canted A-type phase before transforming to the ferromagnetic phase for large  $x$  (close to 1). This is in agreement with recent experiments [8]. Further study is needed in this direction covering the whole doping regime  $0.5 < x < 1$ .

A major drawback of the current approach as well as that of earlier works is the homogeneous magnetic phases they predict. It seems likely that a phase separated regime is energetically more favourable than the canted phase [29]. Phase separation, static or dynamic, seems to be a notable feature of manganites in the low-hole doped regime, charge ordered regime as well as the intermediate regime where there is a ferromagnetic metal to paramagnetic insulator transition as the temperature is varied. Batista *et. al.* [30] through exact diagonalization studies of a single band model on small one dimensional clusters find that non-uniform ground states are highly possible in DE-SE systems. In particular, they find that at low electron doping, doped carriers get trapped at impurity sites and form ferromagnetic clusters. It will be interesting to study the two-band model to find exact nature of the G-phase near  $x = 1$ . We expect the ferromagnetic clusters to be anisotropic in size with ' $x - y$  radius' being larger than the ' $z$  radius'. It should be possible to study phase separation using an orbitally degenerate version of the continuum model proposed by Soto *et. al.* [31]. It is also possible that the spiral [32] and the flux phases [33] get stabilized for some values of doping as in the case of a single band double-exchange model though in our mean field picture we have not considered these phases. Work along these lines is in progress and will be reported elsewhere.

To compare our results with the earlier work, we find a G-phase for low electron doping. We also find that the region over which the G-phase is stabilized increases with  $J_{AF}/t$ . This feature survives when canting is included as the canting angle is small for finite  $J_H/t$ . Our mean field theory takes into account the canting of core spins and also results in the A-phase near  $x = 0.5$  (as seen in experiments) both of which are missing in the work of Maezono *et. al.* [13]. Our model concentrates on the minimum number of relevant parameters and gives a unified picture of the electron-doped manganites (including bilayers). This is in sharp contrast to the work of Maezono *et. al.* which uses five dimensionless parameters and separate order parameters for magnetic and orbital ordering. Our mean field theory also reproduces the C-phase between  $x = 0.6$  and  $x = 0.9$  which is missing in the strong coupling limit of Sheng and Ting [26]. We also clarified the nature of the G-phase near  $x = 1$  and the G-C phase boundary is as expected on physical grounds in contrast to van den Brink and Khomskii [14].

In conclusion we have studied a model for electron-doped manganites with super-exchange between  $t_{2g}$  elec-

trons and double-exchange between orbitally degenerate  $e_g$  electrons. We find that finite  $J_H$  changes the phase diagram qualitatively. In particular the G-phase is favoured for low electron doping. This happens because the *finite* -  $J_H$  model, by allowing electrons to hop to neighbouring sites at an energy cost of  $J_H$  reduces the canting making the phase resemble more to the G-phase. The phase diagram agrees very well with the experimental phase diagram of manganites for  $0.5 < x < 1$ . By extending our mean field theory to incorporate the CE phase we find that it is stabilized over a wide range of values of  $J_H S_0/t$  and  $J_{AF} S_0^2/t$  at  $x = 0.5$ . We extended this model for a two-layer system to predict the magnetic phase diagram of electron doped bilayer manganites. Here we find that the reduced dimensionality washes out the C-type phase. We also notice that the kinetic energy gain due to DE leads to selective orbital ordering in the A and C phases while it is absent in the G-phase. We conclude that the present model qualitatively explains the anisotropic magnetic phases and believe that it can describe the phase transitions between these structures under an external field. A detailed study of this model is called for which should reveal the speculation about the phase separation in electron doped manganites.

## VIII. ACKNOWLEDGEMENTS

I thank T.V.Ramakrishnan for discussions, critical comments and his encouragement, R. Mahendiran for discussions and comments, A. Pande for a careful reading of the manuscript, M. Mithra for help with figures, CSIR (India) for support and SERC (IISc, Bangalore) for computational resources.

---

\* *email* : venkat@physics.iisc.ernet.in

- [1] A. P. Ramirez, *Jl. Phys. Cond. Matter* **9**, 8171 (1997).
- [2] J. M. D. Coey, M. Viret and S. von Molnar, *Adv. in Physics* **48**, 167 (1999).
- [3] T. V. Ramakrishnan, in *Colossal Magnetoresistance, Charge Ordering and Related Properties of Manganese Oxides* ed. by C.N.R. Rao and B. Raveau, World Scientific (1998).
- [4] In this paper we use the term electron-doping for compounds with  $x > 0.5$ . This should not be confused with doping  $AMnO_3$  with a tetravalent ion such as Ce.
- [5] T. Akimoto, Y. Maruyama, Y. Moritomo, A. Nakamura, K. Hirota, K. Ohoyama and M. Ohashi, *Phys. Rev. B* **57**, R5594 (1998).
- [6] R. Kajimoto, H. Yoshizawa, H. Kawano, H. Kuwahara, Y. Tokura, K. Ohoyama and M. Ohashi, *Phys. Rev. B* **60**, 9506 (1999).

- [7] E. O. Wollan and W. C. Koehler, Phys. Rev. **100**, 545 (1955).
- [8] R. Mahendiran, private communication.
- [9] S. Satpathy, Z. S. Popović and F. R. Vukajlović, Phys. Rev. Lett. **76**, 960 (1996).
- [10] Y. Moritomo, A. Asamitsu, H. Kuwahara and Y. Tokura, Nature **380**, 141 (1996).
- [11] Our results cannot be applied to systems such as  $\text{La}_{1-x}\text{Ca}_x\text{MnO}_3$  for which the C-phase extends over a large range of doping.
- [12] R. Mahendiran, M. R. Ibarra, A. Maignan, C. Martin, B. Raveau and C. Ritter, manuscript under preparation.
- [13] R. Maezono, S. Ishihara and N. Nagaosa, Phys. Rev. **B 57**, R13993 (1998).
- [14] J. van den Brink and D. Khomskii, Phys. Rev. Lett. **82**, 1016 (1999).
- [15] Though the  $J_H \rightarrow \infty$  limit explains several experiments well, e.g., the low temperature magnon spectrum, finite  $J_H$  effects are also important. For example, the interband transitions observed in optical conductivity measurements are between bands spin-split by a gap of  $O(J_H)$ . This happens because the energy scales of  $J_H$  and  $W$  are comparable in these systems which can also be inferred from electronic band structure calculations.
- [16] P. W. Anderson, Phys. Rev. **115**, 2 (1959); K. I. Kugel and D. Khomskii, Sov. Phys. JETP **37**, 725 (1973).
- [17] When canting is included, we define the C-phase as fully ferromagnetic in  $z$  direction, the A-phase as fully ferromagnetic in  $x-y$  plane and the G-phase as the structure with spins canted from isotropic antiferromagnet. However, [14] defines the A-phase with  $\cos\theta_{xy} > \cos\theta_z$  and the C-phase with  $\cos\theta_{xy} < \cos\theta_z$  where  $\theta_{xy}$  and  $\theta_z$  are the canting angles.
- [18] A. J. Millis, P. B. Littlewood and B. I. Shraiman, Phys. Rev. Lett. **75**, 5144 (1995).
- [19] D. Feinberg, P. Germain, M. Grilli and G. Seibold, Phys. Rev. **B 57**, R5583 (1998).
- [20] G. Venketeswara Pai, under preparation.
- [21] H. Y. Hwang, P. Dai, S-W. Cheong, G. Aeppli, D. A. Tennant and H. A. Mook, Phys. Rev. Lett **80**, 1316 (1998).
- [22] The precise value of  $J_H/t$  is hard to obtain. Various values have been used in the literature. We follow [9] and S. K. Mishra, R. Pandit and S. Satpathy, Phys. Rev. **B 56**, 2316 (1997).
- [23] J. van den Brink, G. Khaliullin and D. Khomskii, Phys. Rev. Lett. **83**, 5118 (1999).
- [24] T. Hotta Y. Takada, H. Koizumi and E. Dagotto, Phys. Rev. Lett. **84**, 2477 (2000).
- [25] S. Yunoki, T. Hotta and E. Dagotto, Phys. Rev. Lett. **84**, 3714 (2000).
- [26] L. Sheng and C. S. Ting, *cond-mat/9812374*.
- [27] P. D. Battle, M. A. Green, N. S. Laskey, J. E. Millburn, P. G. Radaelli, M. J. Rosseinsky, S. P. Sullivan and J. F. Vente, Phys. Rev. **B 54**, 15967 (1996).
- [28] R. Maezono and N. Nagaosa, Phys. Rev. **B 61**, 1825 (2000).
- [29] A. Moreo, S. Yunoki and E. Dagotto, Science **283**, 2034 (1999).
- [30] C. D. Batista, J. Eroles, M. Avignon and B. Alascio, Phys. Rev. **B 58**, R14689 (1998).
- [31] J. M. Román and J. Soto, Phys. Rev. **B 59**, 11418 (1999).
- [32] J. Inoue and S. Maekawa, Phys. Rev. Lett. **74**, 3407 (1995).
- [33] M. Yamanaka, W. Koshibae and S. Maekawa, Phys. Rev. Lett. **81**, 5604 (1998).

Fig(1) : Phase diagram of the double-exchange and super-exchange model with degenerate  $e_g$  orbitals assuming the doped electrons go into the  $\Gamma$  point and there is no canting of the core spins. (a) Phase diagram as a function of  $J_{AF}S_0^2/t$  for a fixed value of  $J_H S_0/t = 5$ . (b) Phase diagram as a function of  $J_H S_0/t$  for a fixed value of  $J_{AF}S_0^2/t = 0.053$ .

Fig(2) : Phase diagram of the double-exchange and super-exchange model with degenerate  $e_g$  orbitals for a fixed value of  $J_H S_0/t = 5$ . Depending on the electron doping concentration and the ratio of the  $t_{2g}$  superexchange to the  $e_g$  bandwidth,  $J_{AF}S_0^2/t$ , we find the A-type, C-type, G-type or ferromagnetic order. Values of  $J_H$ ,  $t$  and  $J_{AF}$  were taken from density functional calculation[9].

Fig(3) : Phase diagram of the double-exchange and super-exchange model with degenerate  $e_g$  orbitals for a fixed value of  $J_{AF}S_0^2/t = 0.053$ . Depending on the electron doping concentration and the ratio of the Hund's coupling to the  $e_g$  bandwidth,  $J_H S_0/t$  we find the A-type, C-type, G-type or ferromagnetic order. Values of  $J_H$ ,  $t$  and  $J_{AF}$  were taken from the density functional calculation[9].

Fig(4) : Phase diagram of the double-exchange and super-exchange model with degenerate  $e_g$  orbitals at  $x = 0.5$ .

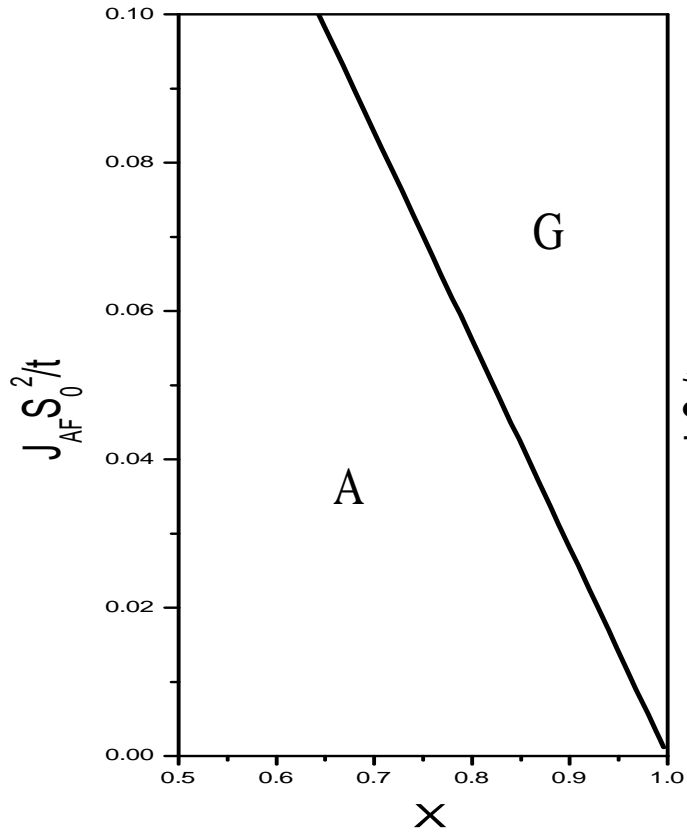
Fig(5) : The angle difference between the neighbour spins (in radians) for a representative value of doping  $x = 0.98$  and  $J_{AF}/t = 0.053$  as a function of  $J_H/t$ .

Fig(6) : Phase diagram of the bilayer system for a fixed value of  $J_H S_0/t = 5$ . Depending on the electron doping concentration and the ratio of the  $t_{2g}$  superexchange to the  $e_g$  bandwidth,  $J_{AF}S_0^2/t$ , we find the A-type, G-type or ferromagnetic order. Note that the C-phase is missing in the bilayer system.

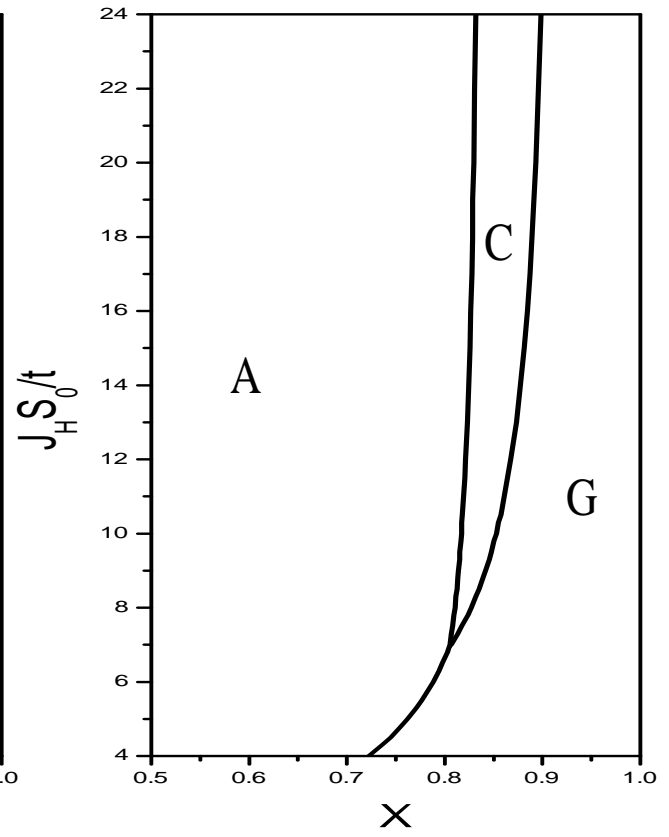
Fig(7) : Phase diagram of the bilayer system for a fixed value of  $J_{AF}S_0^2/t = 0.053$ . Depending on the electron doping concentration and the ratio of the Hund's coupling to the  $e_g$  bandwidth,  $J_H S_0/t$  we find the A-type or G-type phases.







(a)



(b)

Fig. 1

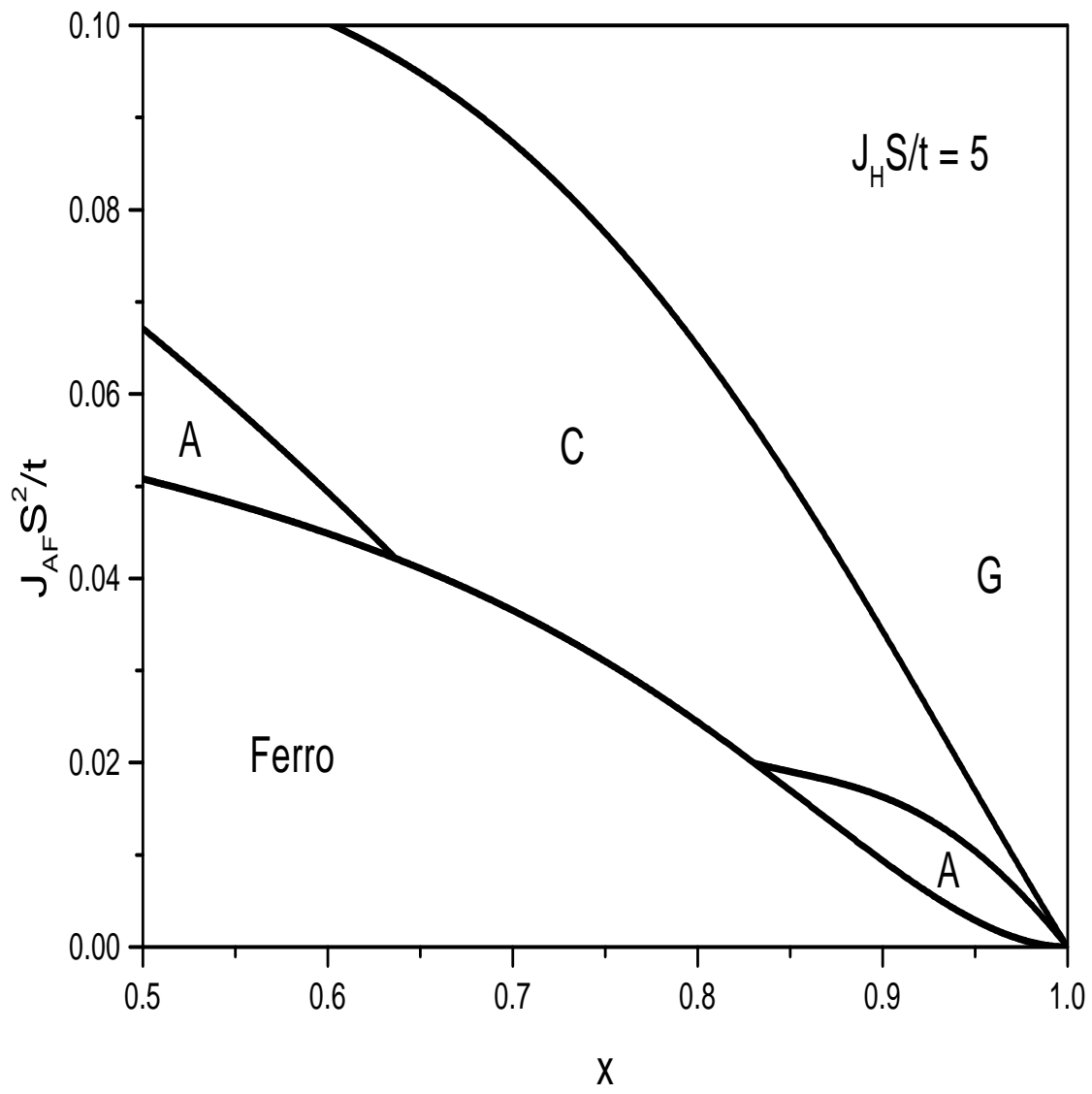


Fig. 2

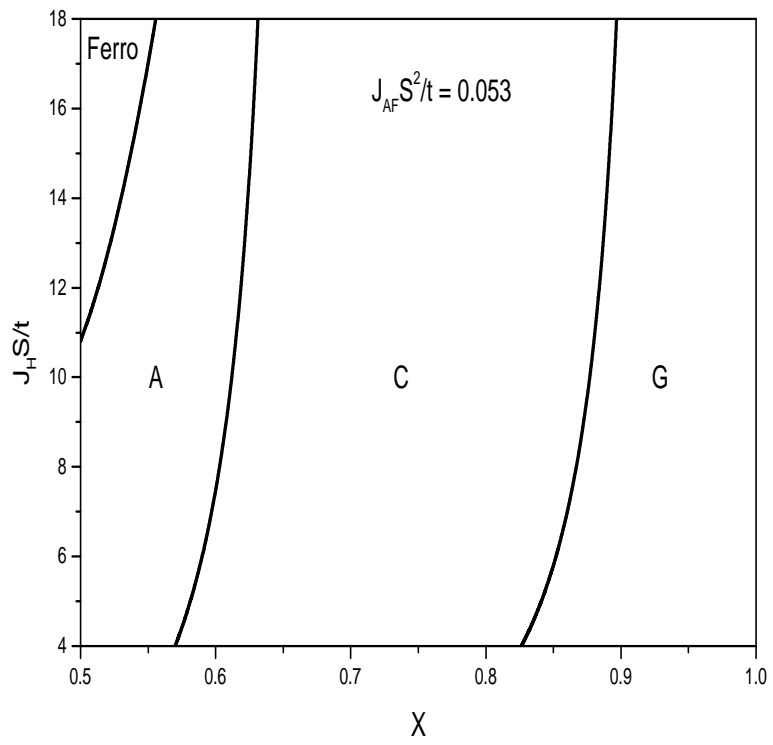


Fig. 3

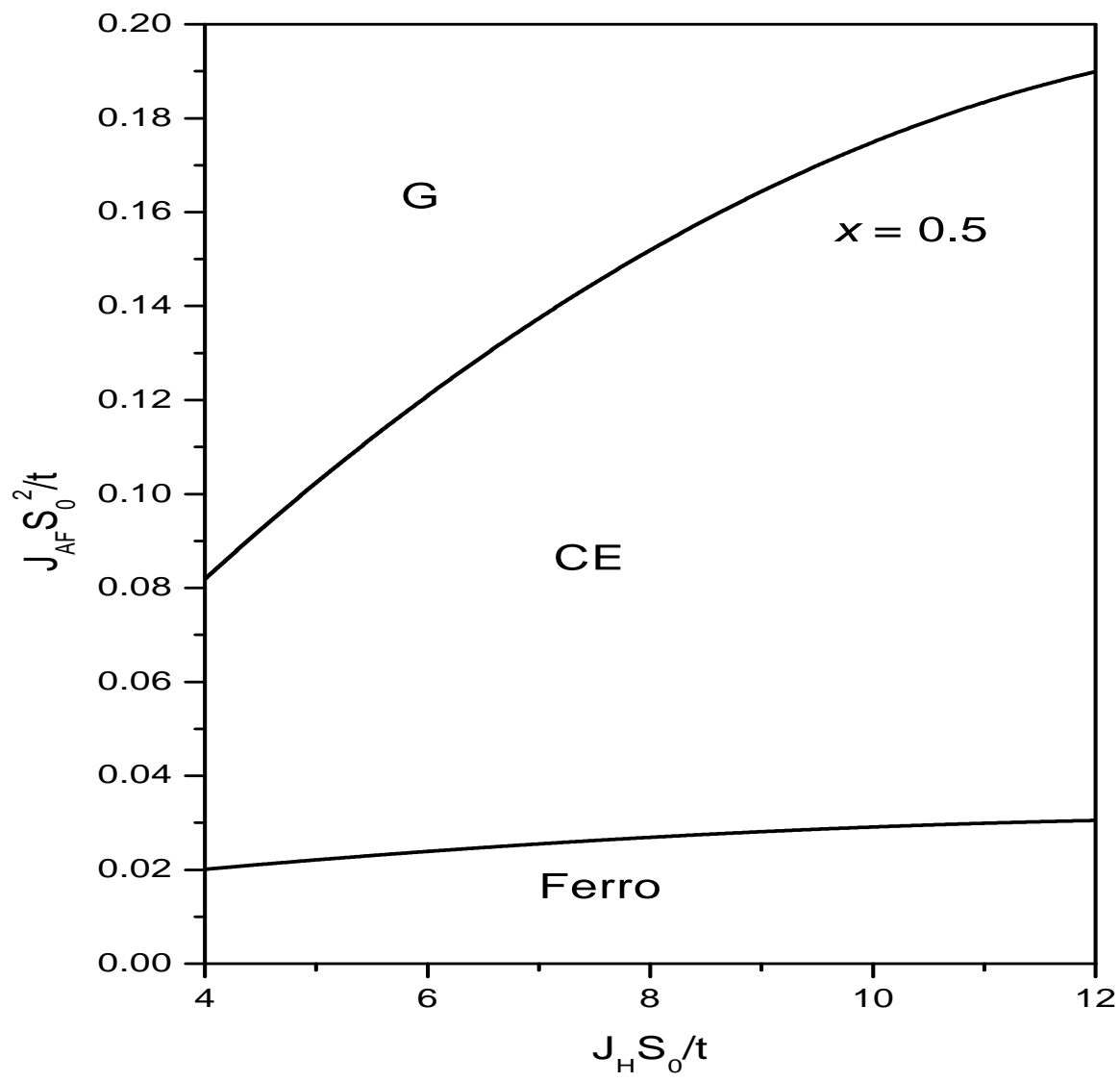


Fig. 4

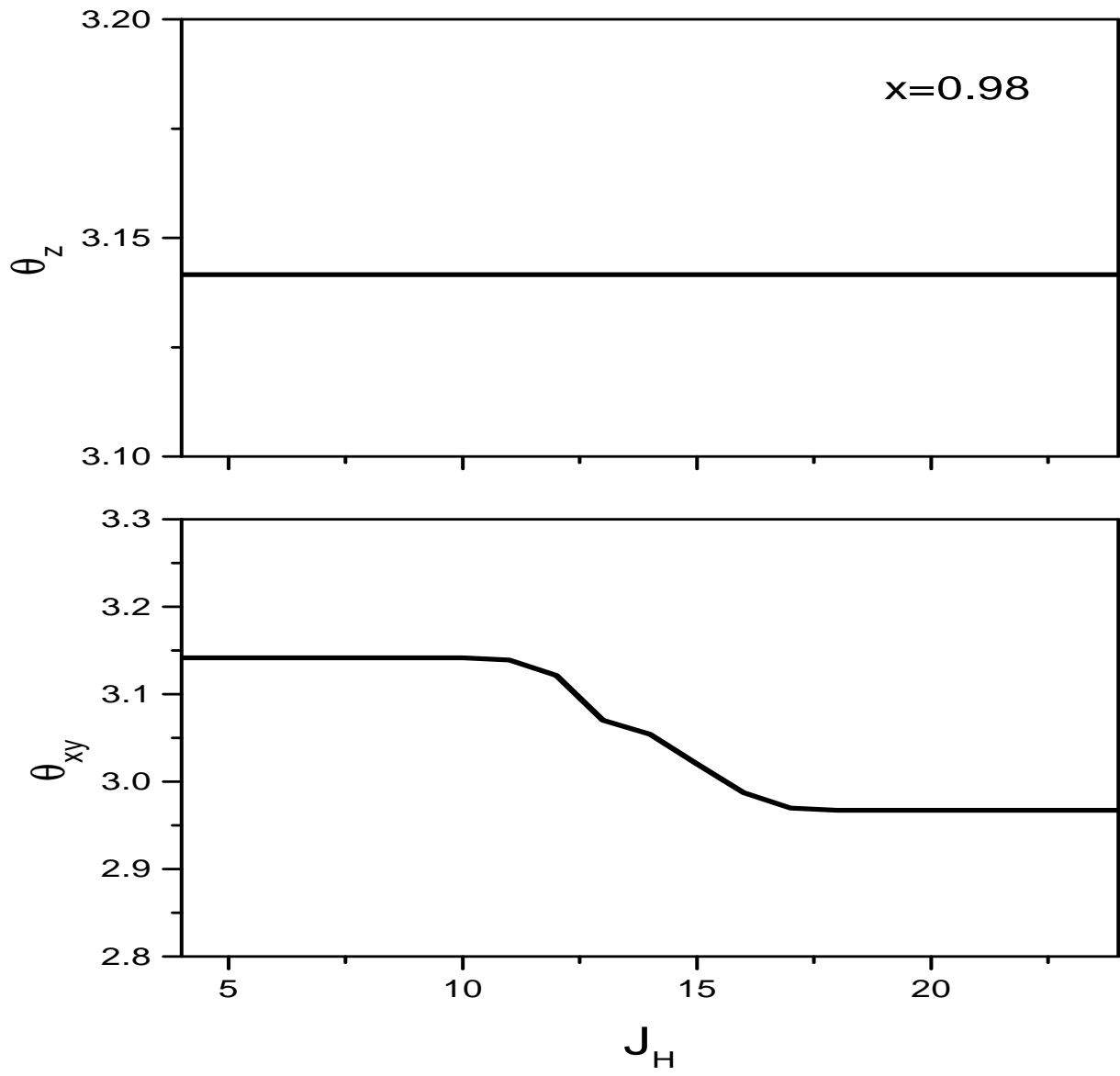


Fig. 5

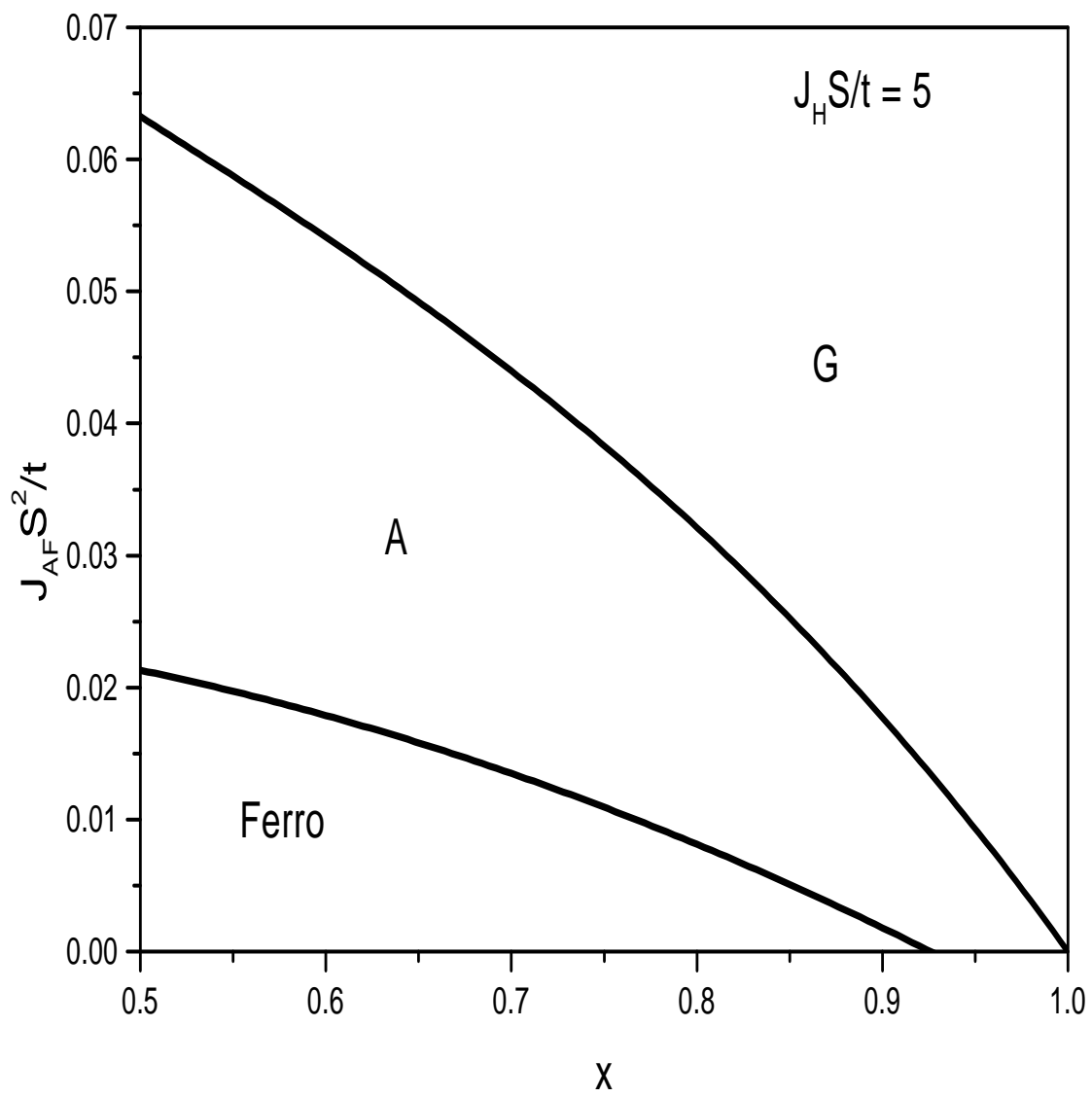


Fig. 6

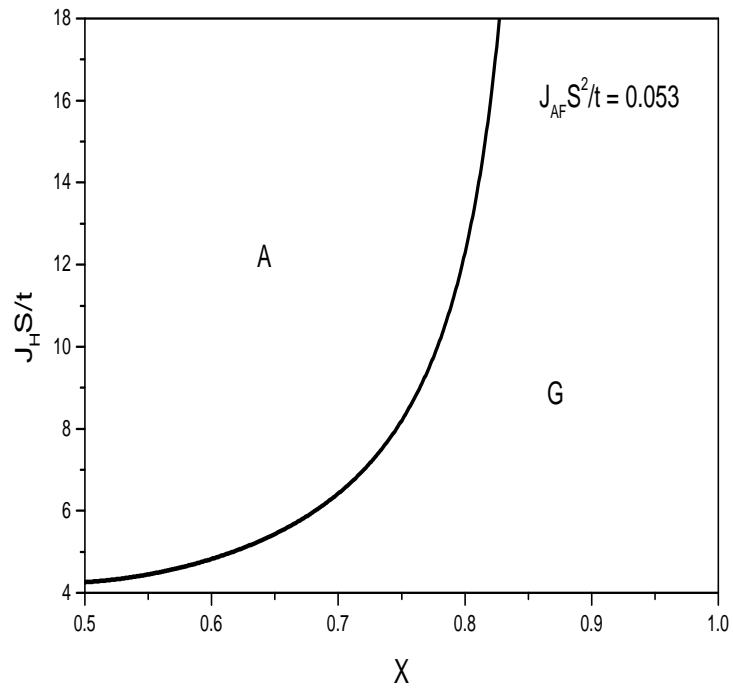


Fig. 7